Hydrol. Earth Syst. Sci. Discuss., https://doi.org/10.5194/hess-2018-146
Manuscript under review for journal Hydrol. Earth Syst. Sci.
Discussion started: 29 March 2018

Hydrology and Earth System Sciences
Discussions

Inundation mapping based on reach-scale effective geometry

Cédric Rebolho[1], Vazken Andréassian[1], and Nicolas Le Moine[2]

[1]Irstea, UR HYCAR, 1 Rue Pierre-Gilles de Gennes, 92160 Antony, France
[2]Sorbonne Universités, UPMC Univ Paris 06, CNRS, EPHE, UMR 7619 Metis, 4 Place Jussieu, 75005 Paris, France

Correspondence to: Cédric Rebolho (cedric.rebolho@irstea.fr)

Abstract. The production of spatially accurate representations of potential inundation is often limited by the lack of available data as well as model complexity. We present in this paper a new approach for rapid inundation mapping, MHYST, which is well adapted for data-scarce areas; it is based on hydraulic geometry concepts for channels, and on DEM data for floodplains. Its originality lies in the fact that it does not work at the cross section scale but computes effective geometrical properties to describe the reach scale. Combining reach-scale geometrical properties with 1-D steady-state flow equations, MHYST computes a topographically coherent relation between the "Height Above Nearest Drainage" and streamflow. This relation can then be used on a past or future event and produce inundation maps. The MHYST approach is tested here on an extreme flood event that occurred in France in May-June 2016. The results indicate that it has a tendency to slightly underestimate inundation extents, although efficiency criteria values are clearly encouraging. The spatial distribution of model performance is discussed and it shows that the model can perform very well on most reaches, but has difficulties modelling the more complex, urbanised reaches. MHYST should not be seen as a rival to detailed inundation studies, but as a first approximation able to rapidly provide inundation maps in data-scarce areas.

1 Introduction

Floods are a recurring phenomenon in France: in September 2014, intense rainfall affected the south of the country, leading to several deaths and about 0.6 billion euros worth of damage. The following year, in October, about 20 people died in the south-east due to massive flooding, which caused a loss of half a billion euros. Then, in June 2016, large-scale flooding occurred over the Seine and Loire catchments, mainly affecting their tributaries and resulting in four deaths at a cost of 1.4 billion euros. These are only examples which underline the value of flood inundation mapping to anticipate the impact of such events. Public authorities and insurance companies are showing a growing interest in the field of rapid inundation modelling, and for the development of simple methods, that would work for any river with easily available data.

Flood hazard assessment usually combines rainfall observations or simulations, a hydrological model, streamflow simulations or observations, and an inundation model in order to generate inundation extents, height maps and sometimes other information (e.g. velocities). Traditionally, flood inundation models are derived from the Shallow Water Equations (SWE) in one or two dimensions (the so-called hydraulic models), with various simplifications that have proved to give satisfying results. For instance, the Regional Flood Model (RFM), probably one of the most comprehensive approaches published so far, is made of four parts (Falter et al., 2014): a daily distributed rainfall-runoff model, a 1D hydraulic model for channel routing, a 2D

hydraulic model for floodplain mapping and a flood loss estimation model. Its application on the Mulde catchment in Germany (Falter et al., 2015) showed mixed results concerning inundation extents, correctly predicting only 50% of the flooded area for the August 2002 event. This underestimation was explained by dike breaches that were not accounted for within the model. Lack of observed data did not allow validation on other events.

Not all hydraulic models need have this degree of complexity. It is indeed possible to neglect specific parts of the SWE depending on the situation. Usually, 2D models use the complete Saint-Venant equations while 1D models often disregard one or several terms, leading, for instance, to the diffusive wave or kinematic wave approximations (e.g. Moussa and Cheviron, 2015). Some methods choose to couple 1D and 2D models, the former for streamflow routing and the latter for overbank flow (Morales-Hernández et al., 2016). Despite the accuracy of such models, studies often try to further simplify them because of the large computing time to simulate small areas and the lack of precise data required to run these models.

LISFLOOD-FP (Bates and De Roo, 2000), a hydraulic model developed to simulate floodplain inundation, was used in several studies (Horritt and Bates, 2001; Hunter et al., 2005; Biancamaria et al., 2009). The model offers different possibilities: using 2D equations or 1D equations decoupled on a 2D grid with kinematic, diffusive or inertial approximations (Bates et al., 2010). Horritt and Bates (2002) published a comparison between different models with gradually increasing complexities (1D, 1D on 2D grid and 2D) and, surprisingly, showed that the 1D model had a better ability to reproduce the two events that were used in validation. The subsequent analysis concluded that the reach studied was relatively narrow and could easily be modelled using simple methods, and the authors argued that the other models would be more appropriate for more complex reaches.

However, these examples concern relatively small and well-instrumented reaches and assessing flood hazard at a larger scale may require different approaches. Alfieri et al. (2014) applied LISFLOOD-ACC, an inertial version of LISFLOOD-FP with decoupled 1D equations on a 100-m resolution grid over Europe in order to map flood hazard for a 100-years return period, assuming a constant return period along the reaches. Broadly speaking, the model splits rivers into small reaches, to apply the hydraulic models independently and to merge simulated maps together, but only for rivers with a catchment larger than 500 km^2. The model was then validated against regional and national hazard maps for six catchments in Germany and the United Kingdom and showed a general over-prediction. Another variation of LISFLOOD-FP for large-scale flood inundation modelling was introduced by Neal et al. (2012), including a new subgrid representation of channel networks for improved model accuracy (Neal et al., 2012; Schumann et al., 2013).

Le Bihan et al. (2017) developed an approach aimed at the forecasting context, in order to cope with excessive computing times. The solution chosen was to run a simple 1D hydraulic model during a "pre-analysis phase" and create a catalogue of inundation extents corresponding to various return periods. These maps are then used, in a forecasting context, to give an estimate of the level of flooding, depending on the forecast discharge.

The lack of precise data (especially for channel cross sections) and the computing time required by numerical methods for solving the SWE motivated the development of potentially alternative methods, mostly based on DEM analysis. For instance, the Rapid Flood Spreading Method (RFSM, Gouldby et al., 2008) chose to divide floodplains into impact zones of different elevations in order to explore the effects of dike breaches using a spilling algorithm based on water depth. Other methods derive

Hydrol. Earth Syst. Sci. Discuss., https://doi.org/10.5194/hess-2018-146
Manuscript under review for journal Hydrol. Earth Syst. Sci.
Discussion started: 29 March 2018

Hydrology and Earth System Sciences
Open Access
EGU
Discussions

inundation maps from topographic information only: one can cite EXZECO (Pons et al., 2010), which introduces elevation noise in the DEM in order to create a single map of "maximum flow accumulation" that can be seen as a potential inundation area, and HAND (Height Above Nearest Drainage), a descriptor originally used for terrain classification (Rennó et al., 2008; Nobre et al., 2011), which has recently been adapted to static flood inundation mapping (Nobre et al., 2016) and is increasingly used to produce flood maps (e.g. Afshari et al., 2018; Speckhann et al., 2018). HAND calculates the difference between river cells' elevation and that of the connected floodplain cells, thus giving relative height information which can be compared to observed flood depths and the corresponding inundation extent.

MHYST, the method presented in this paper, is a simplified approach developed with the aim of rapidly producing inundation maps in data-scarce areas. It combines (i) concepts of hydraulic geometry to characterise channel geometry and (ii) DEM-derived relative elevations to characterise the floodplain; it does not work at the cross section scale but computes effective geometrical properties representative of the reach scale. Combining reach-scale geometrical properties with simplified steady-state hydraulic laws allows one to rapidly generate flood inundation maps while ensuring reach-scale coherence. After describing the method and the validation dataset, MHYST is compared against the inundation extent observed for the major event that occurred in May-June 2016 in France. The last section discusses the spatial distribution of performance and the impact of uncertainties on the results obtained.

2 MHYST : a simplified steady-state hydraulic approach

The MHYST model stands for *Modélisation HYdraulique simplifiée en écoulement STationnaire*, i.e., *Simplified Steady-state Hydraulic Modelling*. It is a flood inundation model which aims to map inundation extents at the reach scale. Where classic hydraulic models use cross sections, this method is based on an effective geometry representative of each river reach. Since no detailed geometric data were available to describe the shape and roughness of the channel river bed for this study, a subgrid representation of the channel was derived from hydraulic geometry relations linking drainage area with bankfull width and height (Leopold and Maddock, 1953). When discharge exceeds bankfull capacity, the model computes a reach-scale relation between streamflow and the "Height Above Nearest Drainage" (HAND) defined by Nobre et al. (2016). This relation can finally be used to assess which height corresponds to the given streamflow, and thus to derive the corresponding inundation map.

2.1 Processing of DEM: from elevations to Height Above Nearest Drainage

The initial step consists in processing the Digital Elevation Model (DEM) in order (i) to obtain a flowing Drainage Direction map (we used the Flow Direction function from ESRI ArcGIS), (ii) to identify the subcatchments (corresponding to the river reaches), and (iii) to compute the Height Above Nearest Drainage (HAND) in each subcatchment. This initial processing is the basis of the floodplain analysis in MHYST.

Figure 1 shows the procedure used to compute HAND values: for a given floodplain cell, it is the difference between its elevation and that of the closest river cell in terms of drainage direction. For instance, the cell of elevation 25 at the top of the

Hydrol. Earth Syst. Sci. Discuss., https://doi.org/10.5194/hess-2018-146
Manuscript under review for journal Hydrol. Earth Syst. Sci.
Discussion started: 29 March 2018

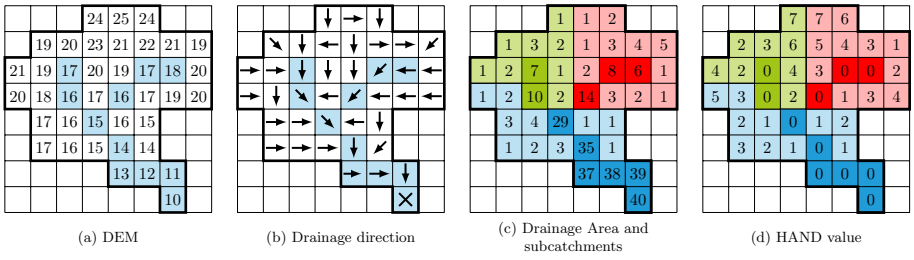

Figure 1. Processing of DEM and calculation of the HAND value for a hypothetical catchment.

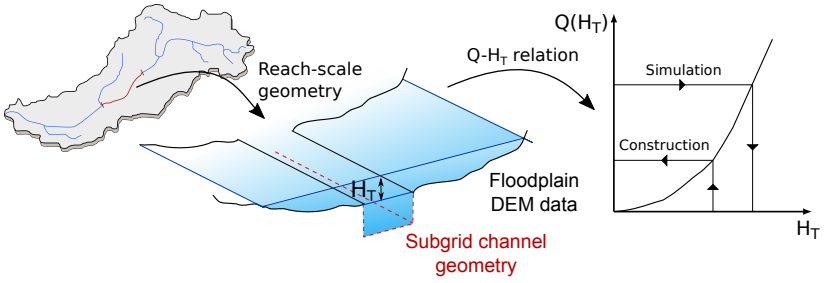

Figure 2. Representation of the model structure: the reach-scale geometry is derived from hydraulic geometry relations and DEM data and is then used to compute a relation between the threshold height H_T and the discharge Q. L is a fixed characteristic of the reach.

figure is linked to (i.e. flows towards) the most upstream red river cell which has an elevation of 18: thus, its HAND value is $25 - 18 = 7$. This relative height has been used as a proxy for inundation height by various studies (Nobre et al., 2016; Afshari et al., 2018). To derive an inundation map from HAND values, we must define a threshold height H_T: the flooded area corresponds to all the cells whose HAND value is strictly lower than H_T (Jafarzadegan and Merwade, 2017).

2.2 Model description

MHYST is mostly based on a DEM and its derivatives (drainage map and drainage areas) and on the hydraulic equations describing a steady uniform flow at the reach scale. This means that for a given time-step (day in this case), at a given reach, we make the approximation that the flow is constant over time and space (this is obviously a strong simplification that we will discuss later). Table 1 sums up the variables used in the following equations as well as their respective units and interpretations. Table 2 describes the two free parameters of the model. The following equations show the path to build a reach-scale relation between H_T and the streamflow Q by calculating, with hydraulic formulas, the discharge value corresponding to a given H_T. Once this relation is known, the model can easily simulate a hydrological event by inverting the relation, and by searching for which H_T corresponds to the given Q (Fig. 2).

Hydrol. Earth Syst. Sci. Discuss., https://doi.org/10.5194/hess-2018-146
Manuscript under review for journal Hydrol. Earth Syst. Sci.
Discussion started: 29 March 2018

Hydrology and Earth System Sciences
Discussions
Open Access
EGU

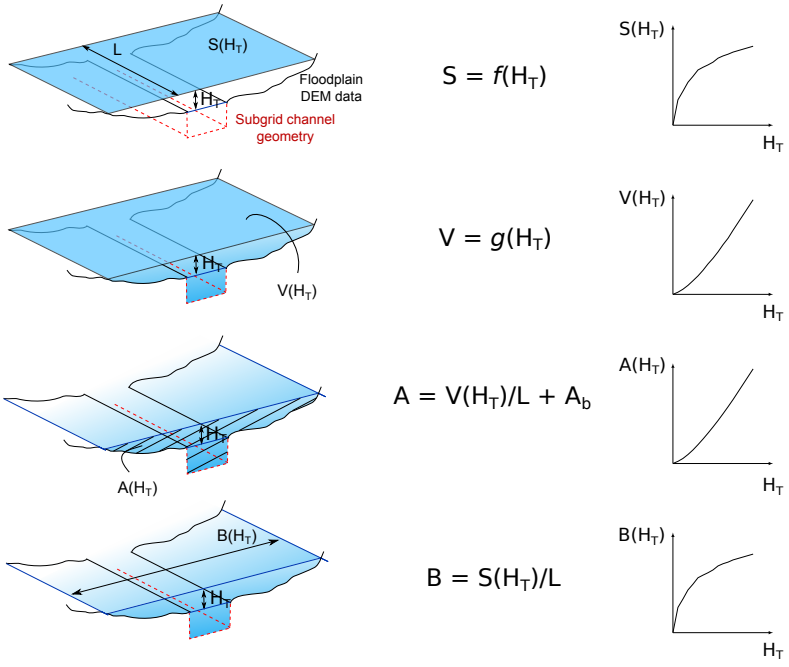

Figure 3. Representation of the reach-scale geometry derived from HAND and the DEM. $A(H_T)$ and $B(H_T)$ are derived from $V(H_T)$ and $S(H_T)$ respectively (Eq. 1 and 2).

Other variables can be directly calculated from the DEM (Fig. 3): for a given threshold height H_T at a reach of length L (L is a fixed parameter of the model), $V(H_T)$ is the sum of volumes above all flooded pixels and $S(H_T)$ is the area occupied by the flooded cells. $A(H_T)$, in Eq. 1, is the average cross section area of the flooded reach and it depends on $V(H_T)$ and on the bankfull cross section area of the channel ($A_b = h_b \cdot W_b$). This variable can also be defined as the sum of the channel cross section area ($A_{ch} = A_b + H_T \cdot W_b$) and the floodplain cross section area ($A_{fp} = A(H_T) - A_{ch}$). $B(H_T)$, in Eq. 2, is the average surface width of the flooded reach, defined similarly from $S(H_T)$ and L.

$$A(H_T) = \frac{1}{L} \cdot V(H_T) + A_b = A_{ch} + A_{fp} \tag{1}$$

$$B(H_T) = \frac{1}{L} \cdot S(H_T) \tag{2}$$

The only unknown variables in these equations are subgrid parameters h_b (bankfull water level) and W_b (bankfull width), i.e. the bankfull geometry, which cannot be obtained from usual DEMs and are only available from detailed surveys for a small

Hydrol. Earth Syst. Sci. Discuss., https://doi.org/10.5194/hess-2018-146
Manuscript under review for journal Hydrol. Earth Syst. Sci.
Discussion started: 29 March 2018

number of rivers. This is why we used downstream hydraulic geometry equations to estimate them, assuming a rectangular channel, the size of which depends on the upstream drainage area (Eq. 3 and 4). To assess the coefficients α and β, we used satellite images from the French platform Géoportail in order to link observed bankfull widths and drainage areas. The values found for the Loing catchment are: $\alpha = 0.053$ and $\beta = 0.822$. The other coefficients, δ and ω, were taken from a study by Blackburn-Lynch et al. (2017), which attempted to regionalise these parameters in the U.S. We used the general values found for the whole set of catchments: $\delta = 0.27$ and $\omega = 0.21$. Although these values probably add uncertainties in the model, they are an accessible way to assess bankfull channel geometry and could still be improved by local bankfull studies when available.

$$W_b = \alpha \cdot A_D^{\beta} \tag{3}$$

$$h_b = \delta \cdot A_D^{\omega} \tag{4}$$

The fundamental equations of the MHYST model come from an experimental study by Nicollet and Uan (1979) which defines the DEBORD formulation as in Eqs. 5 to 7. Building on the Manning-Strickler formula, these authors proposed an empirical parametrisation of turbulent momentum exchange between the channel and the floodplain. This formulation expresses the conveyance capacity depending on channel-related and floodplain-related variables. The coefficient C takes into account the interaction of flows between the fast-flowing channel and the slow-flowing floodplain, and the corresponding head losses.

$$De = K_{ch} \cdot C \cdot A_{ch} \cdot R_{ch}^{2/3} + K_{fp} \cdot \sqrt{A_{fp}^2 + A_{ch} \cdot A_{fp} \cdot (1 - C^2)} \cdot R_{fp}^{2/3} \tag{5}$$

$$C = \begin{cases} C_0 = 0.9 \cdot \left(\dfrac{K_{fp}}{K_{ch}}\right)^{1/6} & \text{if } r = \dfrac{R_{fp}}{R_{ch}} > 0.3 \\ \dfrac{1 - C_0}{2} \cdot \cos\left(\dfrac{\pi \cdot r}{0.3}\right) + \dfrac{1 + C_0}{2} & \text{if } 0 \leq r \leq 0.3 \end{cases} \tag{6}$$

$$Q = De \cdot \sqrt{I_f} \tag{7}$$

The streamflow Q is finally defined from the conveyance capacity and the channel slope, since we hypothesise a uniform flow. R_{ch} and R_{fp} can easily be calculated from the assumed reach geometry (Eq. 8 and 9), which only leaves the Strickler coefficients as unknown variables.

$$R_{ch} = \frac{A_{ch}}{W_b + 2 \cdot h_b} \tag{8}$$

$$R_{fp} = \frac{A_{fp}}{B(H_T) - W_b} \tag{9}$$

Hydrol. Earth Syst. Sci. Discuss., https://doi.org/10.5194/hess-2018-146
Manuscript under review for journal Hydrol. Earth Syst. Sci.
Discussion started: 29 March 2018

Hydrology and Earth System Sciences
Discussions

Table 1. Names, units and interpretations of the variables used in the geometric and hydraulic equations of the MHYST model.

Variable	Unit	Interpretation
H_T	m	Threshold height
$V(H_T)$	m^3	Volume created by a height H_T over a reach
$S(H_T)$	m^2	Flooded area created by a height H_T over a reach
$A(H_T)$	m^2	Average cross section area created by a height H_T over a reach
$B(H_T)$	m	Average surface width created by a height H_T over a reach
$Q(H_T)$	$m^3 \cdot s^{-1}$	Mean discharge created by a height H_T over a reach
D_e	$m^3 \cdot s^{-1}$	Conveyance capacity
A_{ch}	m^2	Cross section area of the channel
A_{fp}	m^2	Cross section area of the floodplain
R_{ch}	m	Hydraulic radius of the channel
R_{fp}	m	Hydraulic radius of the floodplain
I_f	$m \cdot m^{-1}$	Slope of the channel
h_b	m	Bankfull water level of the channel
W_b	m	Bankfull width of the channel
A_b	m^2	Bankfull cross section area of the channel
Q_b	$m^3 \cdot s^{-1}$	Bankfull discharge of the channel
A_D	m^2	Drainage area upstream a given cell
L	m	Target length of a reach (fixed)

Table 2. Names, units and interpretations of the free parameters of MHYST's structure.

Parameter	Unit	Interpretation
K_{ch}	$m^{1/3} \cdot s^{-1}$	Strickler roughness coefficient for the channel
K_{fp}	$m^{1/3} \cdot s^{-1}$	Strickler roughness coefficient for the floodplain

The two Strickler coefficients add two degrees of freedom, and K_{ch} is additionally used to calculate the bankfull flow from the Manning-Strickler formula (Eq. 10).

$$Q_b = K_{ch} \cdot \left(\frac{W_b \cdot h_b}{L_b + 2 \cdot h_b} \right)^{2/3} \cdot \sqrt{I_f} \cdot h_b \cdot W_b \tag{10}$$

Here, we sum up the procedure, which operates at the reach scale:

1. For a given threshold height H_T, we use the DEBORD formulation to calculate the corresponding discharge Q.
2. By repeating the operation for all possible H_T, we obtain a reach-specific table matching values of H_T and Q.

Hydrol. Earth Syst. Sci. Discuss., https://doi.org/10.5194/hess-2018-146
Manuscript under review for journal Hydrol. Earth Syst. Sci.
Discussion started: 29 March 2018

3. When working on an event where only Q is known, when it is greater than Q_b (which means that the river overflowed), the model looks for the corresponding H_T value in the table, by calculating a linear interpolation between two values if necessary, and then assigns to each cell in the subcatchment a flooded height $h_{flood} = max(0; H_T - HAND_{\text{cell}})$.

Although this method and that of Zheng et al. (2017) (submitted to JAWRA) were developed independently, they share a lot of similarities, both using HAND to derive a reach-scale geometry which is used as input for a simplified hydraulic model. However, in addition to HAND, MHYST uses downstream hydraulic geometry relations to evaluate a subgrid representation of the channel geometry. The hydraulic model is also different: Zheng et al. (2017) use the Manning-Strickler formula, while MHYST computes streamflow values from the DEBORD formulation.

2.3 Boundary conditions

MHYST can work with either simulated or observed flows. In this paper, observed data from 12 measurement stations of the French HYDRO database (Leleu et al., 2014) were used to create an observed distributed streamflow map by interpolating flows based on drainage area (Eq. 11) for river pixels between outlets:

$$Q = Q_{up} + \frac{A_D - A_{D,up}}{A_{D,down} - A_{D,up}} \times (Q_{down} - Q_{up}) \tag{11}$$

where Q and A_D are the streamflow and drainage area of any river cell between two outlets, Q_{up}, Q_{down}, $A_{D,up}$ and $A_{D,down}$ are the direct upstream and downstream outlet discharges and drainage areas. This way, streamflow is coherently interpolated over the network, and then averaged at the reach scale.

3 Material

3.1 Generic data

In this study, we used a $5-\mathrm{m}$ resolution DEM covering the Loing catchment (Fig. 4) from IGN (the French national institute for geographic information), which was filled and corrected to avoid depressions and to allow a strict coherence of flow directions, meaning that every pixel flows to the sea. Drainage directions and areas were derived from this DEM and used as model inputs along with elevations. The adaptations and modifications of the DEM were conducted using ESRI ArcGIS.

Daily observed discharges were obtained from the French HYDRO database (Leleu et al., 2014) and the stations were used to delineate the hydrological network over the catchment. Validation data for the Loing catchment were obtained from the activation EMSN028 of the Copernicus Emergency Management Service (©2016 European Union). The original Copernicus study covered a small part of the River Seine and half of the Loing catchment (Fig. 5). However, since the study area and the defined river network were smaller, we cropped the inundation extent to match the study area (Fig. 5). These validation data are post-processed observed data, meaning that the original maps came from satellite observations but they were then modified to build a more homogeneous inundation extent, i.e. nearby areas whose elevations were below the observed flood level were

Hydrol. Earth Syst. Sci. Discuss., https://doi.org/10.5194/hess-2018-146
Manuscript under review for journal Hydrol. Earth Syst. Sci.
Discussion started: 29 March 2018

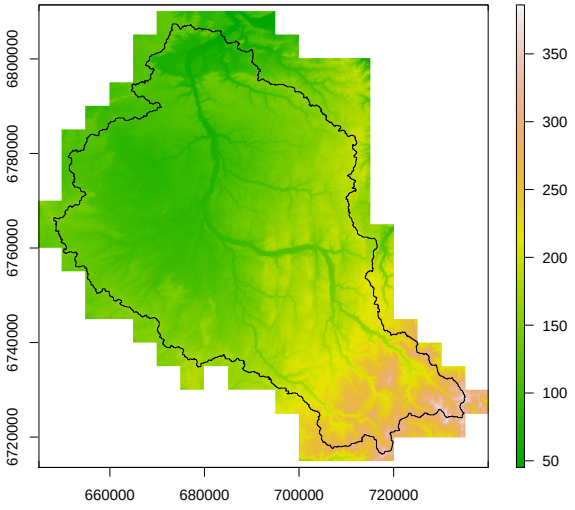

Figure 4. 5 m depressionless DEM used in this study. Elevations go from 45 to 390 m. Corrections have been applied so that each pixel flows to the sea.

added to the inundation extent and merged with all the others. The maximum flood extent was then validated by the European Service against reported flood damage and hydrological measurements (SERTIT, 2016).

3.2 Event of May-June 2016

Following an extremely wet month of May (namely the wettest on record for many stations), a heavy rainfall event started on May 30, 2016 over the center of France, affecting the Upper and Middle Seine basin and the Middle Loire basin. This episode lasted until June 6 and, combined with highly saturated soils due to a series of preceding minor events, led to major flood inundations. Over this period, overall precipitation reached 180 mm in Paris and Orléans, while in some tributaries, such as the River Loing, peak flows largely exceeded those of the record 1910 flood event (Fig. 6). The flood resulted in four deaths, 24 people injured and 1.4 billion euros worth of damage. A total of 1 148 cities were declared in a state of natural disaster and insurance companies received about 182 000 claims (CCR, 2016).

Since validation data were available for June 2016 event, we chose to use our model to simulate this episode and compare the results with observations. We conducted this study over the River Loing, tributary to the River Seine, with a catchment covering 3 900 km^2, a mean elevation of 148 m and a mean slope of 0.03 $m \cdot m^{-1}$. This catchment was heavily impacted by the flood event and concentrates a significant proportion of the inundated area, making it a suitable area to carry out the study. Streamflow data were interpolated from measurements, so no hydrological model is involved in this paper.

Hydrol. Earth Syst. Sci. Discuss., https://doi.org/10.5194/hess-2018-146
Manuscript under review for journal Hydrol. Earth Syst. Sci.
Discussion started: 29 March 2018

Hydrology and Earth System Sciences
Discussions

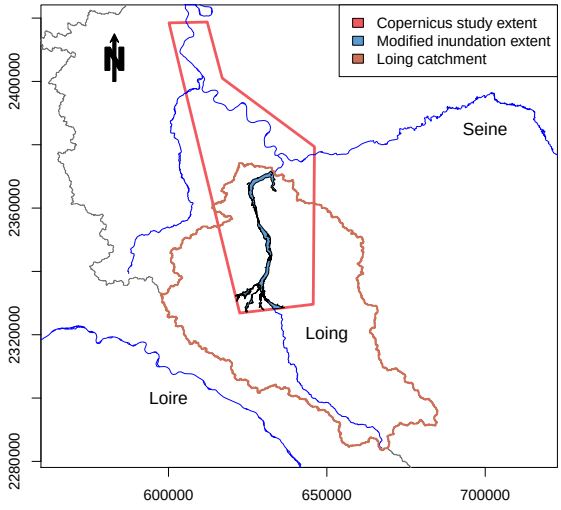

Figure 5. Maximum flood extent for the May-June 2016 event over the Loing catchment produced by the Copernicus Emergency Management Service.

4 Results

4.1 Validation procedure

To assess the model's performance, we used several criteria based on the contingency table in Fig. 7. These scores are presented in detail by Jolliffe and Stephenson (2003) and are defined as a ratio between members of the table where n_1 is the number of hits, i.e. the number of flooded cells correctly forecast, n_4 is the number of pixels correctly forecast as dry, n_2 is the number of false alarms and n_3 the number of observed flooded cells missed by the model. Table 3 summarises the formulas and the interpretations of each score used in this study. These ratios are particularly reliable if they are used to compare simulations and exhaustive observations. This is almost the case with Copernicus validation data which represent a "maximum flood extent". However, MHYST outputs are dated, which is not the case for the observed map. This is why all daily simulated inundation extents were merged into one maximum simulated extent, meaning that we did not try to validate the temporal dynamic of the flood, but only aimed to assess its largest area.

4.2 Parametrisation and validation

MHYST has two free parameters (Table 2): K_{ch} (the Strickler roughness coefficient for the channel) and K_{fp} (the Strickler roughness coefficient for the floodplains). Preliminary studies showed that, for the Loing catchment, a length of $1\,000$ m was a

Hydrol. Earth Syst. Sci. Discuss., https://doi.org/10.5194/hess-2018-146
Manuscript under review for journal Hydrol. Earth Syst. Sci.
Discussion started: 29 March 2018

Hydrology and Earth System Sciences
Discussions

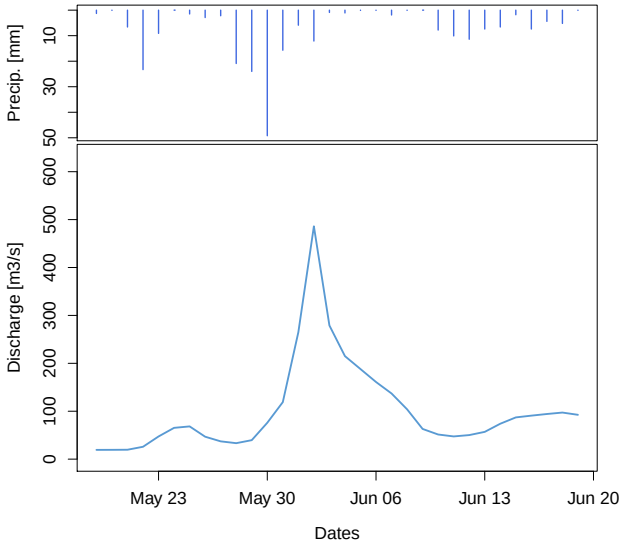

Figure 6. Daily hydrograph of the River Loing at Épisy ($3\,900\ \mathrm{km}^2$) during the event of June 2016. Overall precipitation reached $130\ \mathrm{mm}$. The peak discharge was the largest ever observed on the catchment and reached about $500\ \mathrm{m}^3 \cdot \mathrm{s}^{-1}$.

		Observed	
		Flood	Dry
Model	Flood	Hits (n_1)	False alarms (n_2)
	Dry	Misses (n_3)	Correct negative (n_4)

Figure 7. Contingency table gathering the different scenarios encountered during validation (the numbers refer to pixels).

good trade-off between accuracy and computation time; consequently L was fixed at $1\,000\ \mathrm{m}$ in the rest of this study. K_{ch} and K_{fp} values were tested in the range $[\,0.1\ ;\ 30\,]$ in order to explore a wide range of possibilities (121 combinations were tested).

To help make a decision on the optimal parametrisation of the model, we used the following graphs, on which each (K_{ch}, K_{fp}) couple is characterised by one overall value:

- Two contour plots (Fig. 8) showing the impact of K_{ch} and K_{fp} for the two main scores ($BIAS$ and CSI);

Hydrol. Earth Syst. Sci. Discuss., https://doi.org/10.5194/hess-2018-146
Manuscript under review for journal Hydrol. Earth Syst. Sci.
Discussion started: 29 March 2018

Hydrology and Earth System Sciences
Discussions

Table 3. Table of forecast scores used to assess the performance of a flood simulation. All criteria are based on the contingency table (Fig. 7) and reflect one characteristic of the model. Taken together, they provide a comprehensive analysis of the model's behaviour.

Score	Ratio	Range	Perfect score	Characteristics
Bias ($BIAS$)	$\frac{n_1+n_2}{n_1+n_3}$	$[0,+\infty[$	1	Measures the over-estimation ($BIAS > 1$) and under-estimation ($BIAS < 1$) of the model.
False alarm ratio (FAR)	$\frac{n_2}{n_1+n_2}$	$[0,1]$	0	Fraction of flooded pixels that were actually observed dry. Ignores misses.
Probability of detection (POD)	$\frac{n_1}{n_1+n_3}$	$[0,1]$	1	Proportion of flooded cells intersected by the model. Ignores false alarms.
Critical success index (CSI)	$\frac{n_1}{n_1+n_2+n_3}$	$[0,1]$	1	Counts the number of correct flooded cells, while penalising over-estimation (false alarms) and under-estimation (misses).

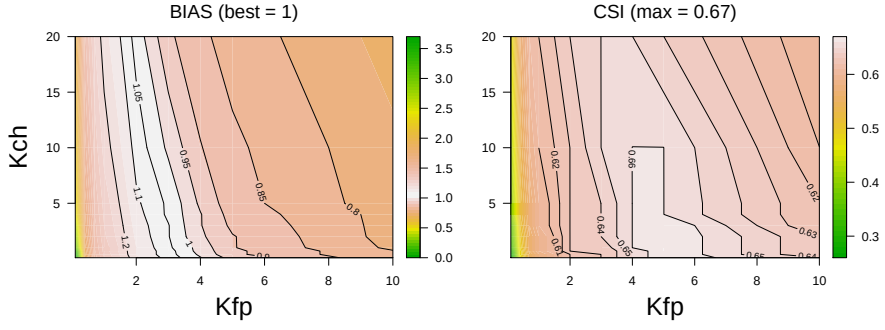

Figure 8. Forecast scores obtained by the model on the River Loing versus Copernicus data for all the parameter values tested.

- A Pareto plot (Fig. 9.a) showing the role played by the K_{fp} parameter in balancing the POD and the FAR;
- A Pareto plot (Fig. 9.b) showing that the CSI identifies the best compromises between the POD and the FAR.

Last, to be able to analyse the variability of results between reaches (we have a total of 90 reaches affected by the inundation), we also computed the CSI and $BIAS$ reach by reach, and produced two cumulative distribution plots showing these results (Fig. 10). We found that:

- The fit criteria are very sensitive to the K_{fp} value and much less to the K_{ch} value (Fig. 8) : this should not be a surprise given that we deal with the maximum flood extents for validation, where K_{ch} only plays a minor role. Remember also that (i) we are modelling a very extreme event ($T \sim 10^3$ years) with substantial overflowing, and (ii) that we are working

Hydrol. Earth Syst. Sci. Discuss., https://doi.org/10.5194/hess-2018-146
Manuscript under review for journal Hydrol. Earth Syst. Sci.
Discussion started: 29 March 2018

Hydrology and Earth System Sciences
Discussions

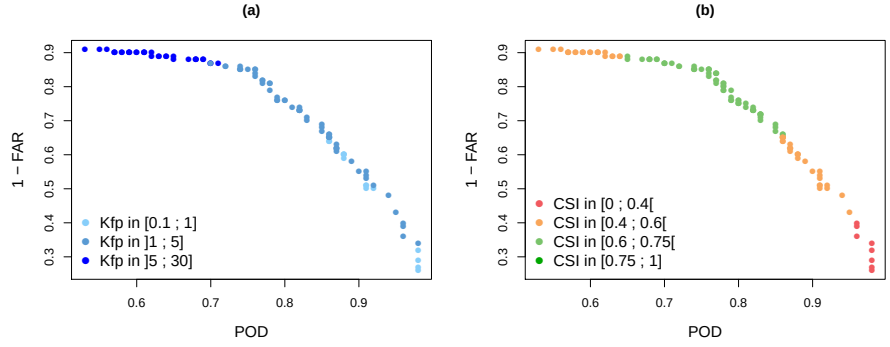

Figure 9. Pareto diagram for two forecast scores, POD and FAR. $1 - FAR$ is used so that each criterion evolves in the same way.

with a channel geometry derived from hydraulic geometry relationships. All this contributes to make the estimation of the channel roughness coefficient more difficult.

– The CSI clearly shows an optimal zone around $K_{fp} = 5$ and $K_{ch} \leq 10\ \mathrm{m}^{1/3} \cdot \mathrm{s}^{-1}$. The best CSI values (greater than 0.66) correspond to combinations where $0.1 \leq K_{ch} \leq 10$ with $K_{fp} = 5$ or $1 \leq K_{ch} \leq 10$ with $K_{fp} = 4$. Given the equifinality, a good way to choose a combination in this range could be to use the most physical one, which, in this case, would be $K_{ch} = 10$ and $K_{fp} = 5\ \mathrm{m}^{1/3} \cdot \mathrm{s}^{-1}$. Indeed, over the catchment, floodplains mainly consist in 44% non-irrigated arable land, 17% broad-leaved forest and 10% pastures with corresponding roughness coefficients reported in the literature of 8, 2 and $4\ \mathrm{m}^{1/3} \cdot \mathrm{s}^{-1}$, respectively (Grimaldi et al., 2010).

– Another way to confirm the validity of this choice ($K_{ch} = 10$ and $K_{fp} = 5\ \mathrm{m}^{1/3} \cdot \mathrm{s}^{-1}$) is to look at how this parametrisation behaves at the reach scale. Given a total of 90 reaches, we can compute the CSI and $BIAS$ criteria for each of them and draw a distribution (Fig. 10): we observe that the "optimal" distribution is unbiased and that it represents a solution among the best available for each percentile, we can thus trust this parametrisation as a relatively "all-terrain" one for the Loing catchment. Figure 11 provides a further illustration with a colour-coded classification of each reach depending on its CSI and $BIAS$ value: we observe that the main difficulties occur around the confluences in the southernmost part of the zone (which also happens to be the most urbanised part of the catchment, with also a waterway interacting with the natural hydrographic network).

Last, Fig. 9 provides a good illustration on how parameter sets interact with the FAR, POD and CSI criteria: choosing from the parameter sets having the best CSI makes it possible to find a compromise between a high POD and a low FAR.

5 Conclusions and outlooks

The objective of this paper was to present and validate a simple hydraulic model for rapid inundation mapping in data-scarce areas. MHYST is based on DEM analyses and simple hydraulic equations, creating a reach-scale relation between the average

Hydrol. Earth Syst. Sci. Discuss., https://doi.org/10.5194/hess-2018-146
Manuscript under review for journal Hydrol. Earth Syst. Sci.
Discussion started: 29 March 2018

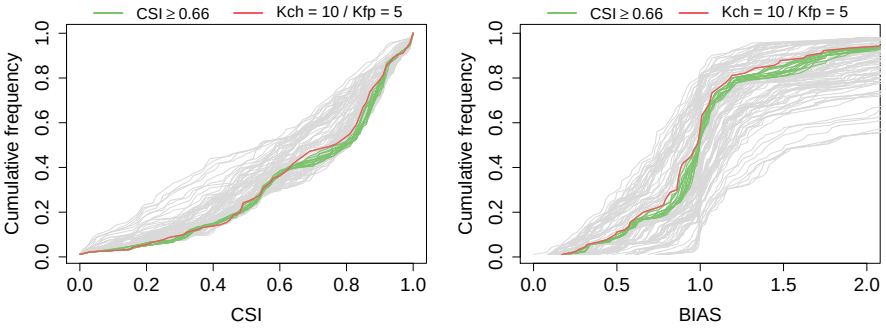

Figure 10. Cumulative frequency of CSI values for all combinations of parameters and for the 90 affected reaches. Green lines correspond to the best combinations identified in Fig. 8 while the red line refers to the physical parametrisation. The other parameters are displayed in grey.

discharge and the average "Height Above Nearest Drainage" which can then be used to simulate any event, past or future, as long as streamflow information (observed or simulated) are available. This model was validated against an observed exceptional flood which occurred in 2016 on the Loing River near Paris and showed results that are certainly not perfect, but from our point of view and for our objectives quite encouraging. The simple structure of MHYST allows it to be used almost anywhere with few data and only two parameters. The model can, however, be used in first approximation, when a lack of time and data restrains the use of a more complex method.

For the sake of honesty, we would like to specify the theoretical limits of the MHYST approach:

- The model equations were solved making the hypothesis of a reach-scale steady uniform flow (probably one of the most simplifying assumptions one can make). This simplification is probably too extreme for highly complex situations, especially in the presence of dikes and bridges. Indeed, on the one hand, the DEM resolution is too coarse to precisely take into account hydraulic structures, and on the other hand, the DEBORD formulation is not sufficient to describe the interaction between the flow and these structures.

- The DEM is a critical part of the model, because geometrical relations and variables are directly related to the shape and distribution of elevations. Another DEM was actually tested as model input and showed much poorer results.

- Moreover, since the channel geometry was unknown, hydraulic geometry equations were used to assess bankfull height and width, with fixed parameters from another study in the case of height, which may not be the optimum for this catchment, adding its share of uncertainty;

- Finally, there is at this point no continuity equation between reaches, since the calculations were made for each reach separately. Uncertainties may therefore be higher in areas around connection points between reaches, especially if it is a confluence of rivers.

Hydrol. Earth Syst. Sci. Discuss., https://doi.org/10.5194/hess-2018-146
Manuscript under review for journal Hydrol. Earth Syst. Sci.
Discussion started: 29 March 2018

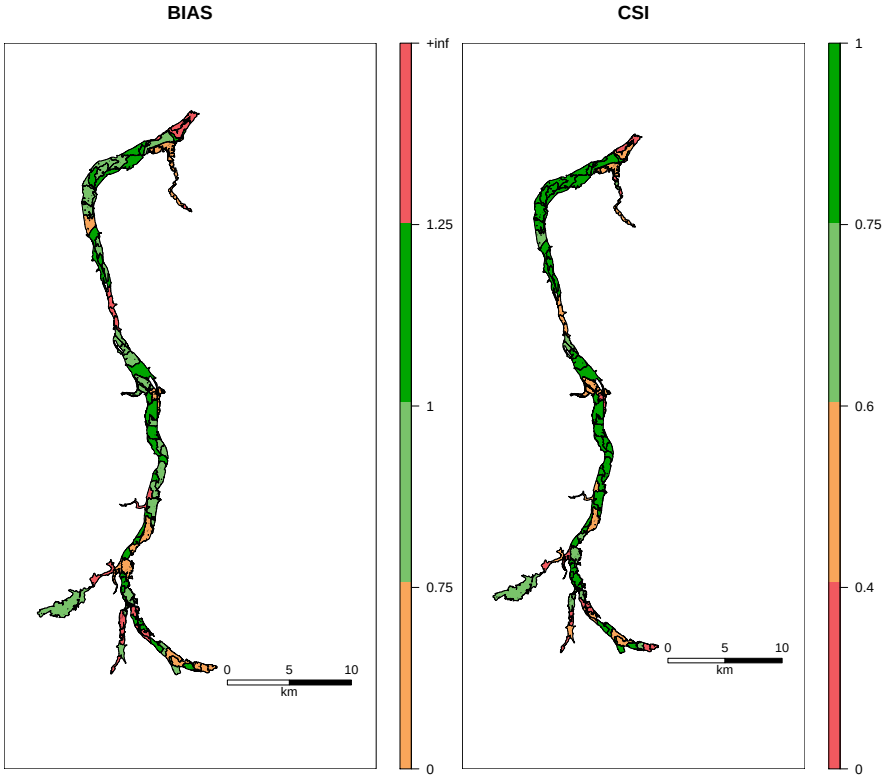

Figure 11. Reach-scale performance for the physycal combination of parameters : $K_{ch} = 10$ and $K_{fp} = 5\ \mathrm{m}^{1/3} \cdot \mathrm{s}^{-1}$. Criteria values have been categorised as follows: excellent (dark green), good (green), average (orange) and poor (red). The black lines delineate the 90 reaches.

Thus, the maps produced by MHYST should be seen as a maximum extent of the flood which can be used as a first and rapid estimation. To further test this approach, we consider that attention should first be given to: assessing the impact of the DEM choice, resolution and quality; testing the approach on a range of (less extreme) events and catchments, to better assess the range and stability of its parameters and performance and improving the treatment of possible discontinuities between reaches.

Data availability. The IGN DEM cannot be freely downloaded.

Copernicus Emergency Management Service data and the corresponding report can be downloaded at:

http://emergency.copernicus.eu/mapping/list-of-components/EMSN028

French observed discharge can be downloaded at:

http://hydro.eaufrance.fr/indexd.php.

Author contributions. The model presented in this paper was developed and analysed by Cédric Rebolho during his PhD work. He also wrote the manuscript which was corrected by Vazken Andréassian and Nicolas Le Moine.

Competing interests. The authors declare that they have no conflict of interest.

Acknowledgements. The first author was funded by a grant from the AXA Research Fund. Thanks are extended to Rafal Zielinksi, who helped us access data from the Copernicus Emergency Management Service. We would also like to thank the AXA Global P&C research team for their advice and our discussions on the development of simple conceptual inundation models. The MHYST model was developed using R (R Core Team, 2015) and GFortran, Gnu compiler collection (gcc) Version 4.9.2.

References

Afshari, S., Tavakoly, A. A., Rajib, M. A., Zheng, X., Follum, M. L., Omranian, E., and Fekete, B. M.: Comparison of new generation low-complexity flood inundation mapping tools with a hydrodynamic model, Journal of Hydrology, 556, 539–556, https://doi.org/10.1016/j.jhydrol.2017.11.036, 2018.

Alfieri, L., Salamon, P., Bianchi, A., Neal, J., Bates, P., and Feyen, L.: Advances in pan-European flood hazard mapping, Hydrological Processes, 28, 4067–4077, https://doi.org/10.1002/hyp.9947, 2014.

Bates, P. D. and De Roo, A. P. J.: A simple raster-based model for flood inundation simulation, Journal of Hydrology, 236, 54–77, https://doi.org/10.1016/S0022-1694(00)00278-X, 2000.

Bates, P. D., Horritt, M. S., and Fewtrell, T. J.: A simple inertial formulation of the shallow water equations for efficient two-dimensional flood inundation modelling, Journal of Hydrology, 387, 33–45, https://doi.org/10.1016/j.jhydrol.2010.03.027, 2010.

Biancamaria, S., Bates, P. D., Boone, A., and Mognard, N. M.: Large-scale coupled hydrologic and hydraulic modelling of the Ob river in Siberia, Journal of Hydrology, 379, 136–150, https://doi.org/10.1016/j.jhydrol.2009.09.054, 2009.

Blackburn-Lynch, W., Agouridis, C. T., and Barton, C. D.: Development of Regional Curves for Hydrologic Landscape Regions (HLR) in the Contiguous United States, JAWRA Journal of the American Water Resources Association, 53, 903–928, https://doi.org/10.1111/1752-1688.12540, 2017.

CCR: Inondations de mai-juin 2016 en France - Modélisation de l'aléa et des dommages, Tech. rep., Service R&D modélisation - Direction des Réassurances & Fonds Publics, 2016.

Falter, D., Dung, N., Vorogushyn, S., Schröter, K., Hundecha, Y., Kreibich, H., Apel, H., Theisselmann, F., and Merz, B.: Continuous, large-scale simulation model for flood risk assessments: proof-of-concept: Large-scale flood risk assessment model, Journal of Flood Risk Management, p. 19, https://doi.org/10.1111/jfr3.12105, 2014.

Falter, D., Schröter, K., Dung, N. V., Vorogushyn, S., Kreibich, H., Hundecha, Y., Apel, H., and Merz, B.: Spatially coherent flood risk assessment based on long-term continuous simulation with a coupled model chain, Journal of Hydrology, 524, 182–193, https://doi.org/10.1016/j.jhydrol.2015.02.021, 2015.

Gouldby, B., Sayers, P., Mulet-Marti, J., Hassan, M. A. A. M., and Benwell, D.: A methodology for regional-scale flood risk assessment, Water Management, pp. 1–14, https://doi.org/10.1680/wama.2008.161.3.169, 2008.

Grimaldi, S., Petroselli, A., Alonso, G., and Nardi, F.: Flow time estimation with spatially variable hillslope velocity in ungauged basins, Advances in Water Resources, 33, 1216–1223, https://doi.org/10.1016/j.advwatres.2010.06.003, 2010.

Horritt, M. S. and Bates, P. D.: Effects of spatial resolution on a raster based model of flood flow, Journal of Hydrology, 253, 239–249, https://doi.org/10.1016/S0022-1694(01)00490-5, 2001.

Horritt, M. S. and Bates, P. D.: Evaluation of 1D and 2D numerical models for predicting river flood inundation, Journal of Hydrology, 268, 87–99, https://doi.org/10.1016/S0022-1694(02)00121-X, 2002.

Hunter, N. M., Horritt, M. S., Bates, P. D., Wilson, M. D., and Werner, M. G. F.: An adaptive time step solution for raster-based storage cell modelling of floodplain inundation, Advances in Water Resources, 28, 975–991, https://doi.org/10.1016/j.advwatres.2005.03.007, 2005.

Jafarzadegan, K. and Merwade, V.: A DEM-based approach for large-scale floodplain mapping in ungauged watersheds, Journal of Hydrology, 550, 650–662, https://doi.org/10.1016/j.jhydrol.2017.04.053, 2017.

Jolliffe, I. T. and Stephenson, D. B.: Forecast Verification: A Practitioner's Guide in Atmospheric Science, John Wiley & Sons, 2003.

Le Bihan, G., Payrastre, O., Gaume, E., Moncoulon, D., and Pons, F.: The challenge of forecasting impacts of flash floods: test of a simplified hydraulic approach and validation based on insurance claim data, Hydrology and Earth System Sciences, 21, 5911–5928, https://doi.org/10.5194/hess-21-5911-2017, 2017.

Leleu, I., Tonnelier, I., Puechberty, R., Gouin, P., Viquendi, I., Cobos, L., Foray, A., Baillon, M., and Ndima, P.-O.: La refonte du système d'information national pour la gestion et la mise à disposition des données hydrométriques, La Houille Blanche, pp. 25–32, https://doi.org/10.1051/lhb/2014004, 2014.

Leopold, L. B. and Maddock, T.: The Hydraulic Geometry of Stream Channels and Some Physiographic Implications, Tech. Rep. 252, Washington, 1953.

Morales-Hernández, M., Petaccia, G., Brufau, P., and García-Navarro, P.: Conservative 1D–2D coupled numerical strategies applied to river flooding: The Tiber (Rome), Applied Mathematical Modelling, 40, 2087–2105, https://doi.org/10.1016/j.apm.2015.08.016, 2016.

Moussa, R. and Cheviron, B.: Modeling of Floods—State of the Art and Research Challenges, in: Rivers – Physical, Fluvial and Environmental Processes, edited by Rowiński, P. and Radecki-Pawlik, A., pp. 169–192, Springer International Publishing, Cham, https://doi.org/10.1007/978-3-319-17719-9_7, 2015.

Neal, J., Schumann, G., and Bates, P.: A subgrid channel model for simulating river hydraulics and floodplain inundation over large and data sparse areas, Water Resources Research, 48, 16, https://doi.org/10.1029/2012WR012514, 2012.

Nicollet, G. and Uan, M.: Écoulements permanents à surface libre en lits composés, La Houille Blanche, pp. 21–30, https://doi.org/10.1051/lhb/1979002, 1979.

Nobre, A. D., Cuartas, L. A., Hodnett, M., Rennó, C. D., Rodrigues, G., Silveira, A., Waterloo, M., and Saleska, S.: Height Above the Nearest Drainage – a hydrologically relevant new terrain model, Journal of Hydrology, 404, 13–29, https://doi.org/10.1016/j.jhydrol.2011.03.051, 2011.

Nobre, A. D., Cuartas, L. A., Momo, M. R., Severo, D. L., Pinheiro, A., and Nobre, C. A.: HAND contour: a new proxy predictor of inundation extent: Mapping Flood Hazard Potential Using Topography, Hydrological Processes, 30, 320–333, https://doi.org/10.1002/hyp.10581, 2016.

Pons, F., Delgado, J.-L., Guero, P., and Berthier, E.: EXZECO : A GIS and DEM based method for pre-determination of flood risk related to direct runoff and flash floods, in: 9th International Conference on Hydroinformatics, Tianjin, CHINA, 2010.

Rennó, C. D., Nobre, A. D., Cuartas, L. A., Soares, J. V., Hodnett, M. G., Tomasella, J., and Waterloo, M. J.: HAND, a new terrain descriptor using SRTM-DEM: Mapping terra-firme rainforest environments in Amazonia, Remote Sensing of Environment, 112, 3469–3481, https://doi.org/10.1016/j.rse.2008.03.018, 2008.

Schumann, G. J.-P., Neal, J. C., Voisin, N., Andreadis, K. M., Pappenberger, F., Phanthuwongpakdee, N., Hall, A. C., and Bates, P. D.: A first large-scale flood inundation forecasting model: Large-Scale Flood Inundation Forecasting, Water Resources Research, 49, 6248–6257, https://doi.org/10.1002/wrcr.20521, 2013.

SERTIT: EMSN-028 Flood delineation and damage assessment, France, Technical Report, 2016.

Speckhann, G. A., Borges Chaffe, P. L., Fabris Goerl, R., Abreu, J. J. d., and Altamirano Flores, J. A.: Flood hazard mapping in Southern Brazil: a combination of flow frequency analysis and the HAND model, Hydrological Sciences Journal, 63, 87–100, https://doi.org/10.1080/02626667.2017.1409896, 2018.

Zheng, X., Tarboton, D., Maidment, D. R., Liu, Y. Y., and Passalacqua, P.: River Channel Geometry and Rating Curve Estimation Using Height Above the Nearest Drainage, submitted to Journal of the American Water Resources Association (JAWRA), 2017.